

Center for Advanced Materials

CAM

Presented at the International Conference on Organic
Materials for Nonlinear Optics, Oxford, England,
June 29-30, 1988

RECEIVED
LAWRENCE
BERKELEY LABORATORY

AUG 31 1988

LIBRARY AND
DOCUMENTS SECTION

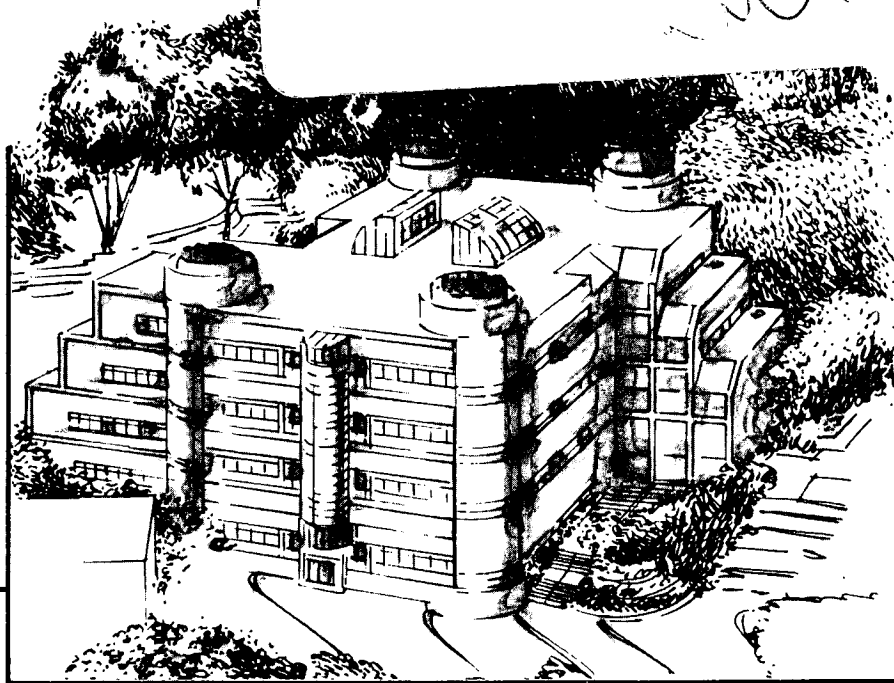
Nonlinear Optical Studies of Organic Monolayers

Y.R. Shen

February 1988

TWO-WEEK LOAN COPY

*This is a Library Circulating Copy
which may be borrowed for two weeks.*



Materials and Chemical Sciences Division
Lawrence Berkeley Laboratory • University of California
ONE CYCLOTRON ROAD, BERKELEY, CA 94720 • (415) 486-4755

LBL-24829
c2

DISCLAIMER

This document was prepared as an account of work sponsored by the United States Government. While this document is believed to contain correct information, neither the United States Government nor any agency thereof, nor the Regents of the University of California, nor any of their employees, makes any warranty, express or implied, or assumes any legal responsibility for the accuracy, completeness, or usefulness of any information, apparatus, product, or process disclosed, or represents that its use would not infringe privately owned rights. Reference herein to any specific commercial product, process, or service by its trade name, trademark, manufacturer, or otherwise, does not necessarily constitute or imply its endorsement, recommendation, or favoring by the United States Government or any agency thereof, or the Regents of the University of California. The views and opinions of authors expressed herein do not necessarily state or reflect those of the United States Government or any agency thereof or the Regents of the University of California.

NONLINEAR OPTICAL STUDIES OF ORGANIC MONOLAYERS

Y. R. Shen

Department of Physics, University of California
Center for Advanced Materials, Lawrence Berkeley Laboratory
Berkeley, California 94720 USA

Second-order nonlinear optical effects are forbidden in a medium with inversion symmetry, but are necessarily allowed at a surface where the inversion symmetry is broken. They are often sufficiently strong so that a submonolayer perturbation of the surface can be readily detected. They can therefore be used as effective tools to study monolayers adsorbed at various interfaces.¹ We discuss here a number of recent experiments in which optical second harmonic generation (SHG) and sum-frequency generation (SFG) are employed to probe and characterize organic monolayers.

We first consider the application of SHG to organic molecular monolayers to measure the nonlinearity of some organic molecules.² As schematically shown in Fig. 1, insoluble amphiphilic molecules can be spread on water in a monolayer form, and their surface density can be controlled by varying the overall surface area. The second harmonic (SH) signal generated from the monolayer is then monitored and compared with that generated from a quartz crystal. From the results, the nonlinear susceptibility $\chi^{(2)}$ for the monolayer relative to that of quartz can be obtained and the nonlinear polarizability $\alpha^{(2)}$ for the molecules can be deduced in the following way.

If the interaction between molecules in the monolayer can be neglected, $\vec{\chi}^{(2)}$ and $N_s \vec{\alpha}^{(2)}$ are simply related by a coordinate transformation from the molecular (ξ, η, ζ) system to the lab (x, y, z) system.³

$$\chi_{ijk}^{(2)} = N_s \langle G_{ijk} \rangle \alpha_{\xi\eta\zeta}^{(2)}, \quad (1)$$

where N_s is the surface density of molecules, $G_{ijk}^{(2)}$ is the

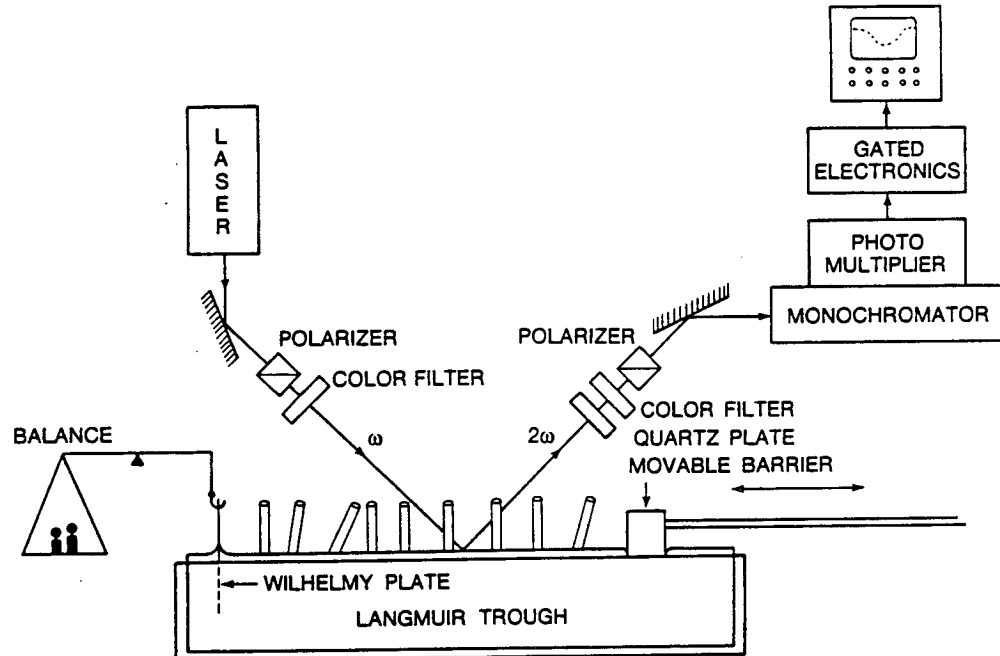


Figure 1 Experimental arrangement for studies of organic monolayers spread on water in a langmuir trough by simultaneous measurements of surface tension and second harmonic generation versus surface area.

transformation matrix, and the angular brackets denote an average over the molecular orientational distribution. In many cases, $\hat{\alpha}^{(2)}$ is dominated by a single element $\alpha_{\xi\xi\xi}^{(2)}$ along the molecular axis ξ , and the molecules have isotropic distribution in the azimuthal plane. One can then easily show that the nonvanishing elements of $\hat{\chi}^{(2)}$ are

$$\begin{aligned} \chi_{zzzz}^{(2)} &= N_s \langle \cos^3 \theta \rangle \alpha_{\xi\xi\xi}^{(2)} \\ \chi_{zxzx}^{(2)} = \chi_{xxzz}^{(2)} = \chi_{zyzy}^{(2)} = \chi_{yzzy}^{(2)} &= \frac{1}{2} N_s \langle \sin^2 \theta \cos \theta \rangle \alpha_{\xi\xi\xi}^{(2)}, \quad (2) \end{aligned}$$

where θ is the angle between $\hat{\xi}$ and the surface normal \hat{z} . With a further assumption of a δ -function for the orientational distribution, measurements of $\chi_{zzzz}^{(2)}$ and $\chi_{zxzx}^{(2)}$ allow us to determine $\alpha_{\xi\xi\xi}^{(2)}$ and θ separately.³

The validity of Eq. (1) means that the local-field correction due to molecule-molecule interaction can be neglected. The analogous relation in the linear case is $\chi_{ij}^{(1)} = N_s \langle G_{ij} \rangle \alpha_{\xi\eta}^{(1)}$ which would imply that the dielectric constant $\epsilon(\omega)$ for the monolayer is close to 1. In our experiment, Eq. (1) can be verified by varying N_s . An example is shown in Fig. 2,² where the square root of the SH signal, which is proportional to $\chi^{(2)}$, is plotted

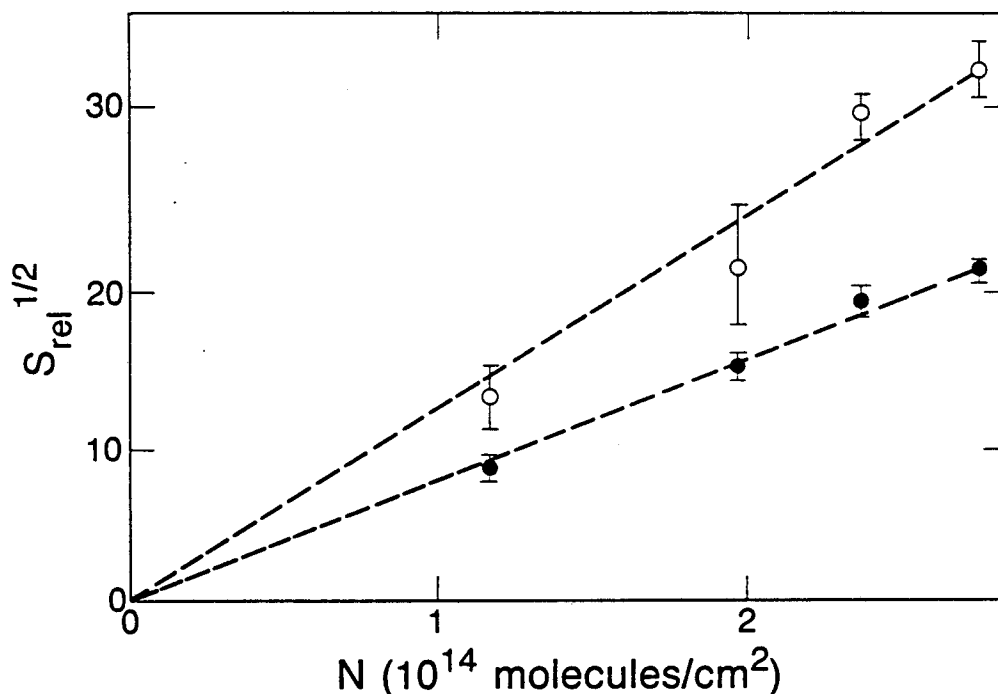


Figure 2 Square root of the relative SHG intensity $S_{rel}^{1/2}$ as a function of surface density for 5CT spread on water. The input laser field was polarized at 45° to the plane of incidence, for which both the s-polarized (open circles) and p-polarized (filled circles) SHG outputs were measured.

against the surface density of 4"-n-pentyl-4-cyano-p-terphenyl (5CT). The linear relation between $\chi^{(2)}$ and N_s is clearly satisfied. With other molecules of higher surface packing densities, deviation from the linear relation has been observed. The local field correction factors must then be included in the calculation.⁴

One can also test experimentally the assumption that $\alpha_{zzz}^{(2)}$ dominates in $\alpha^{(2)}$. If this is not the case, we should find $\chi_{zzxx}^{(2)} \neq \chi_{xxzz}^{(2)}$ and $\chi_{zzyy}^{(2)} \neq \chi_{yyzy}^{(2)}$ even in the low N_s limit. On the other assumption of a δ -function distribution for θ , a crude estimate indicates that it is a good approximation if the spread of θ is less than 10° or if θ is close to 0° or 90° . Finally, $\chi^{(2)}$ for adsorbed molecules is actually compost of three parts:

$$\chi^{(2)} = \chi_{mol}^{(2)} + \chi_{water}^{(2)} + \chi_{int}^{(2)}, \quad (3)$$

where $\chi_{mol}^{(2)}$, $\chi_{water}^{(2)}$, and $\chi_{int}^{(2)}$ are nonlinear susceptibilities due to the molecular monolayer isolated from water, the bare water surface, and the interaction between the

molecules and water, respectively. For organic molecules with relatively high nonlinearity, $\chi_{\text{water}}^{(2)}$ can be neglected. If the molecular properties are not very much affected by the adsorption on water, then $\chi_{\text{int}}^{(2)}$ may also be negligible compared with $\chi_{\text{mol}}^{(2)}$, leaving $\chi^{(2)} = \chi_{\text{mol}}^{(2)}$.

We have used the technique to measure $\alpha_{\xi\xi\xi}^{(2)}$ for a number of structurally related molecules (phenyl derivatives).² The results are what one would normally expect, namely, $\alpha^{(2)}$ increases with the conjugation length and decreases with interruption of electron delocalization by twist between phenyl rings or by replacing phenyl ring by pyrimidine; $\alpha^{(2)}$ also increases with increase of charge transfer.

The above technique used to measure $\alpha^{(2)}$ has the disadvantages that not all molecules can be spread on water and that molecules may have their properties drastically changed when adsorbed on water. The latter is more likely to happen for molecules with large charge transfer between strong electron donor and acceptor end groups. Hemicyanine is an example.⁵ The strong charge-transfer band of

$$R - \text{N}^+ \text{---} \text{---} \text{---} \text{---} \text{N} \text{---} \text{R}'$$
 responsible for the large second-order nonlinearity of the molecule is effectively suppressed by protonation. Adsorption of the molecules on water with only a small amount of acid (~ 0.1% H₂SO₄ by volume) could reduce $\alpha^{(2)}$ of the molecules by more than two orders of magnitude. Special precaution is needed to prevent such changes from happening.

Information deduced from SHG about the orientation of molecular adsorbates is also useful for fundamental understanding of the properties of an organic monolayer. For example, from the SHG measurements, it was found that the liquid expanded-liquid condensed transition of a Langmuir monolayer on water is associated with a sudden change in the molecular orientation.⁶ Since SHG is applicable to any interface accessible by light, it can also be used to study how the orientation of surfactant molecules at liquid/liquid interfaces depends on the environment.⁷ This is relevant, for example, to the understanding of micellar structure. Consider the recent experiment on sodium 1-dodecyl naphthalene-4-sulfonate (SDNS) (C₁₂H₂₅-C₁₀H₆SO₃Na) at C₁₀H₂₂/H₂O and CCl₄/H₂O interfaces. The results yield a polar tilt angle θ of 21° and 38° for SDNA at the two interfaces, respectively, in comparison to $\theta = 13^\circ$ at the air/water interface. Here, the nonlinearity is dominated by $\alpha_{\xi\xi\xi}^{(2)}$ arising from the naphthalene chromophore and the ξ -axis is along the charge-transfer direction from the SO₃ group to the

hydrocarbon chain. The larger θ is qualitatively correlated with the weaker tail-tail interaction of the hydrophobic part of the molecules in the nonaqueous solution due to dielectric screening.

Reactions of molecules in a surface monolayer will change the properties of the monolayer. They can be monitored by SHG. Photo-polymerization of a monolayer is a good example.⁸ The problem is meaningful because two-dimensional polymerization is expected to be very different from the three dimensional one. Moreover, it is now possible to vary the surface density and orientation of the monomers and study their effects on polymerization. Figure 3 describes how the SHG from a monolayer of octadecyl methacrylate (ODMA) on water changes as it is polymerized by UV irradiation. The π electrons associated with the C=C double bond in the monomers contribute significantly to the nonlinearity of the monomers. Upon polymerization, the linkage between monomers changes the double bond to a single bond, and hence reduces the nonlinearity. This explains the decrease of the SH signal with the irradiation time in Fig. 3. The data can be used to test theoretical models for surface polymerization, as shown in Fig. 3.

In some cases, SHG may be too weak to probe a polymer monolayer, but the third-order nonlinearity of the polymer is sufficiently strong so that third harmonic generation (THG) can be used.⁹ For example, a monolayer of poly-4-BCMU (a processable polydiacetylene), yields a TH signal at 0.36 μm that shows an increase in correlation with the conformational transition from a less conjugated yellow form to a more conjugated red form. The surface density at which the transition occurs agrees with the value deduced from the observed transition in the bulk, suggesting that in this case the surface and bulk properties are very much alike.

We can also use SHG to study biologically interesting molecules in monolayer form or embedded in membranes.¹⁰ Retinal chromophores are responsible for vision. These molecules have structures exhibiting a long conjugation length with an appreciable charge transfer. (The all trans retinal, ATR, illustrated in Fig. 4, is a representative example.) One therefore expects a large $\alpha^{(2)}$ for such molecules. Measurements of SHG at 0.266 μm from a monolayer of retinal molecules on water indeed show a value of $\alpha^{(2)}$ larger than 10^{-28} esu. Using the two-band model that relates $\alpha^{(2)}$ with $\Delta\mu$, the difference between the dipole moments of the ground and the excited states, we can then deduce $\Delta\mu$. The latter quantity is important for

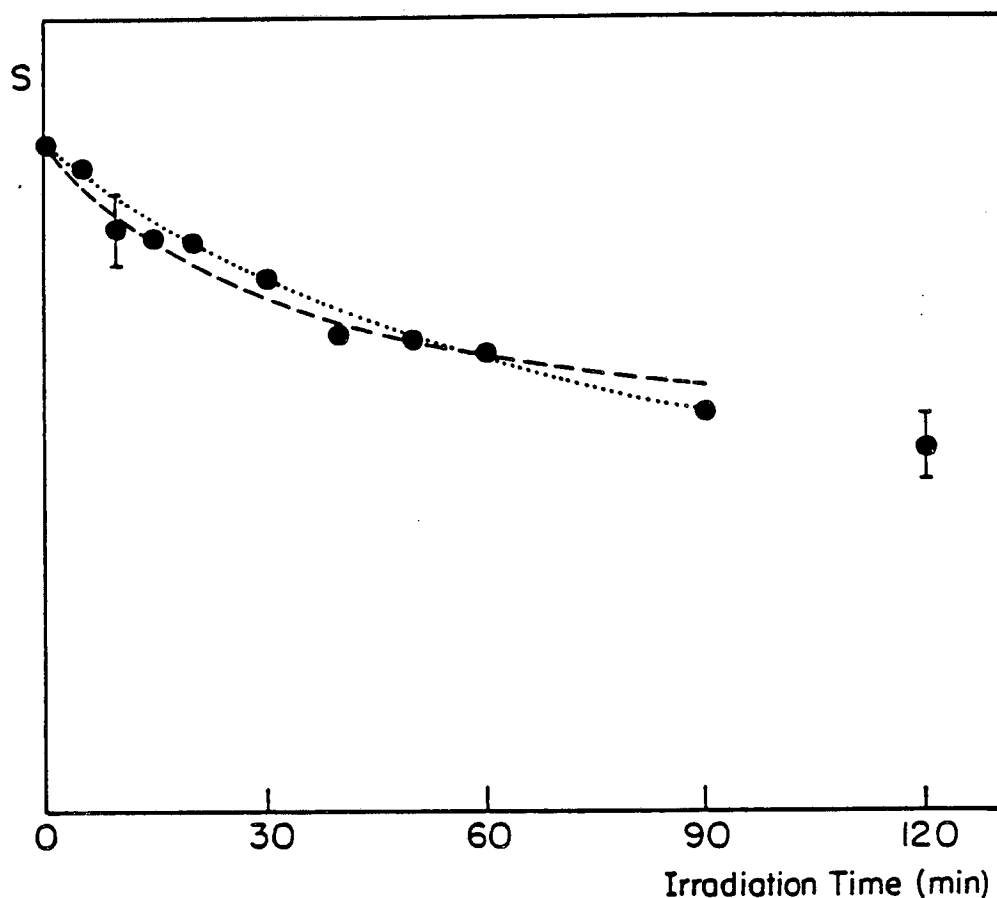


Figure 3 Relative SHG intensity from a monolayer of ODMA on water versus irradiation time for UV polymerization of the monolayer. The dotted and dashed curves are derived from theoretical models assuming first-order and second-order kinetics, respectively.

modeling the photochemistry of vision.

The large value of $\alpha^{(2)}$ would allow the study of retinal chromophores by SHG even when they are embedded in a membrane with a low surface density (but still in polar arrangement). However, it is possible that $\alpha^{(2)}$ may change with environment. A recent SHG experiment on a monolayer of protonated retinylidene n-butylamine Schiff base (PNRB) on water and on PNRB embedded in the purple membrane of *Halobacterium halobium* yielded $\alpha^{(2)}$ for the two cases separately. The results led to nearly the same $\Delta\mu$ for both cases, indicating that $\Delta\mu$ of the chromophore is insensitive to the environment.

By varying the frequency of the input laser, spectral

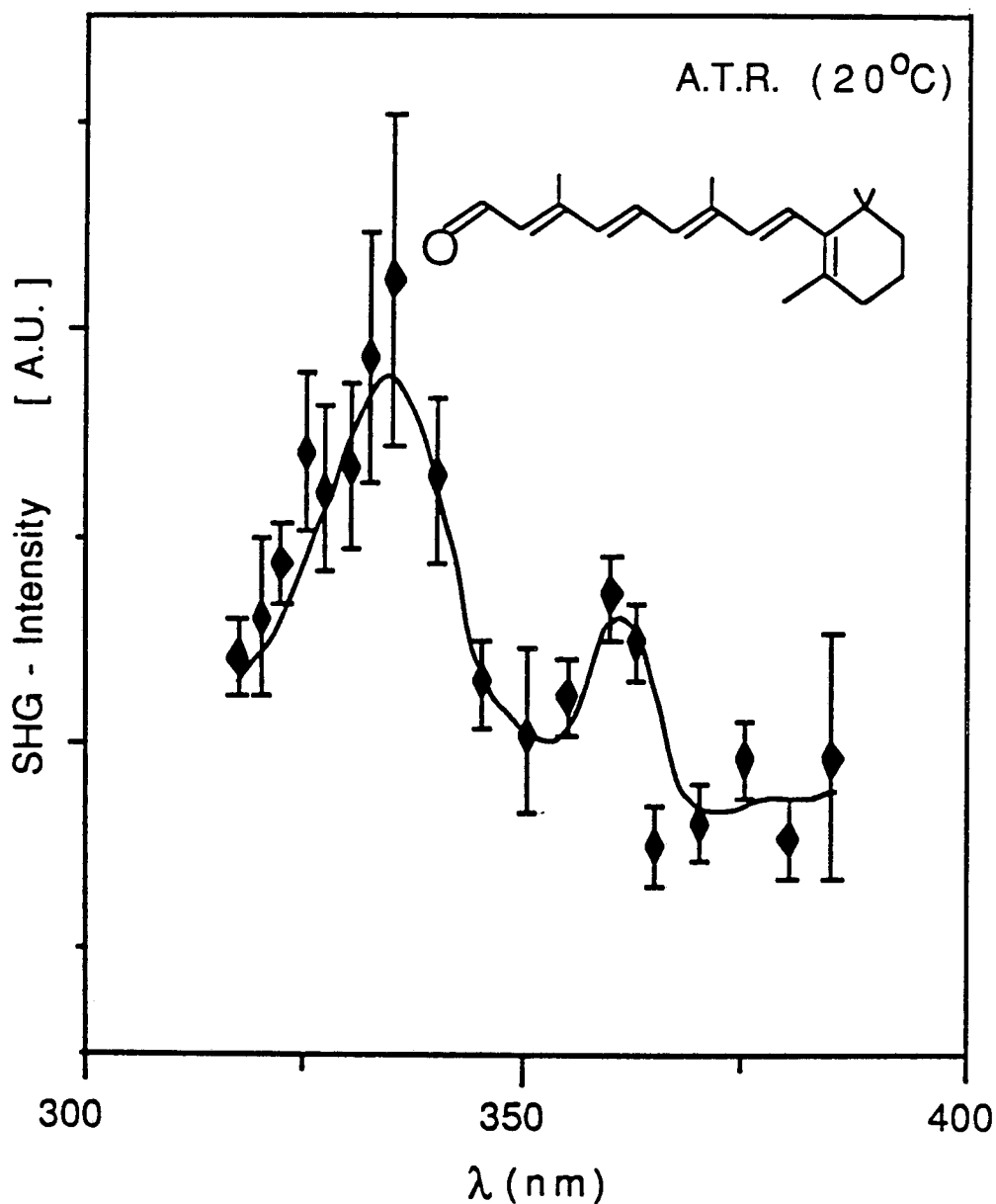


Figure 4 SHG spectrum of a monolayer of all-trans retinal (ATR) at an air/water interface.

information about a retinal monolayer can also be obtained from the SHG measurements.¹⁰ Figure 4 depicts the SH spectrum of a monolayer of ATR on water. Two resonant peaks are seen, one at 335 nm and the other at 360 nm. They can be assigned to one-photon $S_0 \rightarrow B_u$ and two-photon $S_0 \rightarrow A_g$ transitions, respectively, both being blue-shifted from the corresponding ones for ATR in solution.

The monolayer sensitivity of SHG requires the output

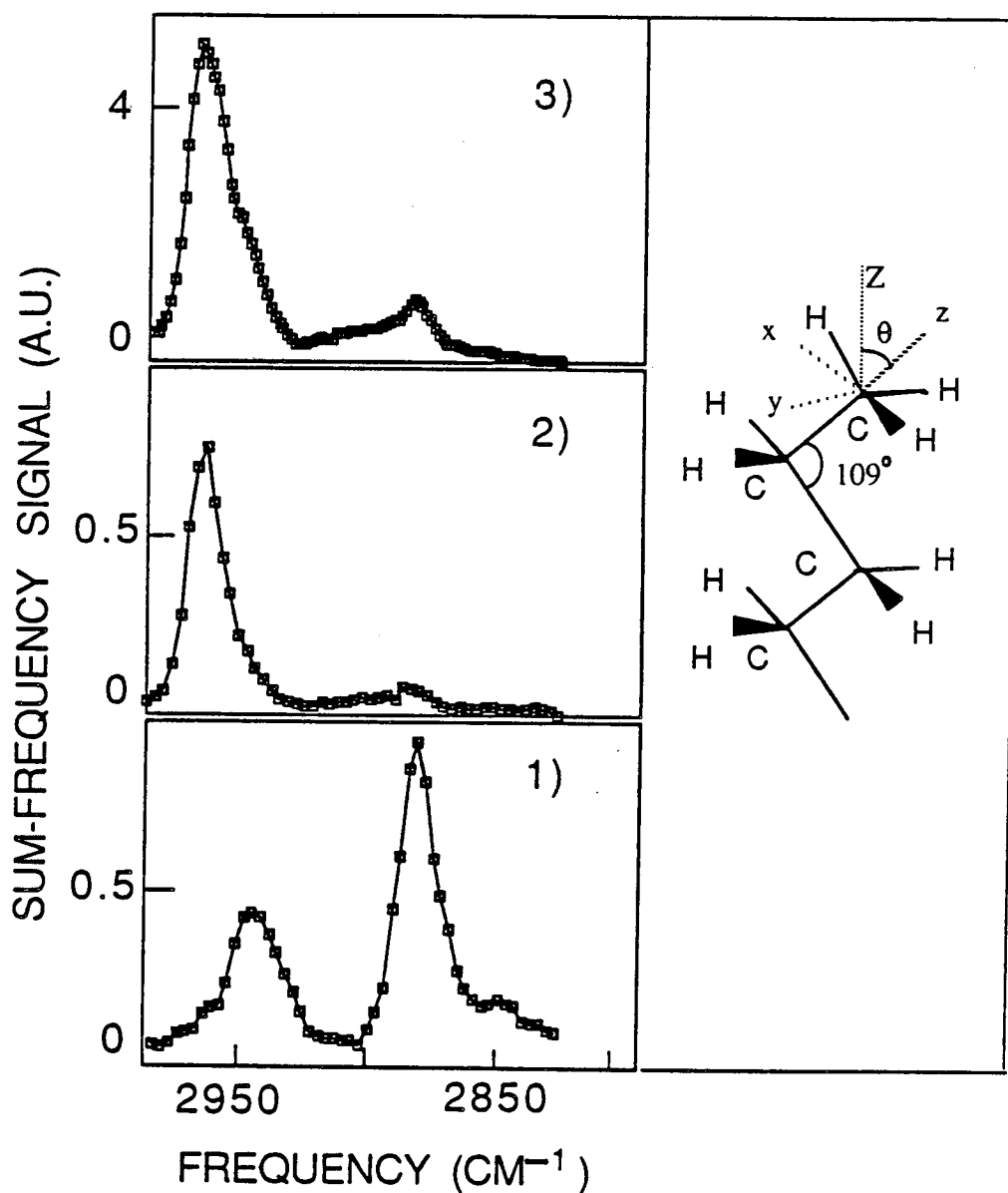


Figure 5 SFG spectra of a full monolayer of PDA with various (vis,IR) polarization combinations: 1) s-visible, p-IR; 2) p-visible, s-IR; 3) p-visible, p-IR. Inset: coordinate axes chosen for the terminal methyl group.

being in the visible so that high-gain photodetectors can be used. For spectroscopic studies, this limits the applications to probing of electronic transitions in molecules. An extension of SHG to sum-frequency generation (SFG), however, removes the limitation. In SFG for surface vibrational spectroscopy, two laser beams are simultaneously incident on the sample, one in the infrared

and the other in the visible. The output at $\omega_1 + \omega_2$ is then also in the visible. Being a second-order process, SFG is as surface-specific as SHG. Tuning of the infrared input then makes surface IR spectroscopy possible.¹¹

Figure 5 shows the SF spectra of the CH stretch modes of a full monolayer of pentadecanoic acid (PDA) on water.¹² All three peaks in the spectra originate from the CH₃ terminal group of the molecules. Because of symmetry, the CH₂ groups give little contribution. The three spectra in Fig. 5 were obtained with different polarization combinations. We mentioned earlier that the results of SHG with different polarizations can be used to deduce information about the molecular orientation. Here, with SFG, we can be even more specific: it is now possible to determine the orientation of a particular group of atoms in a molecule, e.g., the terminal CH₃ group of the long alkane chain of PDA in the present case. The data in Fig. 5 yield an angle $\theta = 35^\circ$ between the symmetry axis of the CH₃ group and the surface normal. This indicates that the alkane chain of PDA is parallel to the surface normal, as expected.

Like SHG, SFG can be applied to any interface accessible by the input beams. Surface monolayer vibrational spectroscopy of adsorbates at air/metal, air/semiconductor and liquid/solid interfaces using infrared-visible sum-frequency generation has already been demonstrated.¹³⁻¹⁵ Monitoring the adsorption kinetics of selected molecular species by SFG has also been found possible.¹⁵

We have shown in this paper the wide applicability of SHG and SFG to organic monolayers. Further applications are limited only by one's imagination.

This work was supported by the Director, Office of Energy Research, Office of Basic Energy Sciences, Materials Sciences Division of the U.S. Department of Energy under Contract No. DE-AC03-76SF00098.

REFERENCES

1. See, for example, Y. R. Shen. Ann. Rev. Mater. Sci., 1986, 16, 69.
2. G. Berkovic, Th. Rasing, and Y. R. Shen, J. Opt. Soc. Amer., 1987, B4, 945.
3. T. F. Heinz, H. W. K. Tom, and Y. R. Shen, Phys. Rev. A, 1983, 28, 1883.
4. P. Ye and Y. R. Shen, Phys. Rev. B, 1983, 28, 4288.

5. G. Marowsky, L. F. Chi, D. Mobius, R. Steinhoff, Y. R. Shen, D. Dorsch, and B. Riger, Chem. Phys. Lett. (to be published).
6. Th. Rasing, Y. R. Shen, M. W. Kim, and S. Grubb, Phys. Rev. Lett., 1985, 55, 2903.
7. S. G. Grubb, M. W. Kim, Th. Rasing, and Y. R. Shen, Langmuir, 1988, 4, 452.
8. G. Berkovic, Th. Rasing, and Y. R. Shen, J. Chem. Phys., 1986, 85, 7374.
9. G. Berkovic, R. Superfine, P. Guyot-Sionnest, Y. R. Shen, and P. Prasad, J. Opt. Soc. Amer. B, 1988, 5, 668.
10. J. Huang, A. Lewis, and Th. Rasing, J. Phys. Chem. (to be published); Th. Rasing, J. Huang, A. Lewis, T. Stehlin, and Y. R. Shen, (to be published).
11. X. D. Zhu, H. Suhr, and Y. R. Shen, Phys. Rev. B, 1987, 35, 3047; J. H. Hunt, P. Guyot-Sionnest, and Y. R. Shen, Chem. Phys. Lett., 1987, 133, 189.
12. P. Guyot-Sionnest, J. H. Hunt, Y. R. Shen, Phys. Rev. Lett., 1987, 59, 1597.
13. A. L. Harris, C. E. D. Chidsey, N. J. Levinos, and D. N. Loiacono, Chem. Phys. Lett., 1987, 141, 350.
14. R. Superfine, P. Guyot-Sionnest, J. H. Hunt, C. T. Kao, and Y. R. Shen, Surf. Sci. Lett. (in press).
15. P. Guyot-Sionnest, R. Superfine, J. H. Hunt, and Y. R. Shen, Chem. Phys. Lett., 1988, 144, 1.

LAWRENCE BERKELEY LABORATORY
TECHNICAL INFORMATION DEPARTMENT
UNIVERSITY OF CALIFORNIA
BERKELEY, CALIFORNIA 94720